MHD Free Convection and Mass Transfer Flow past a Vertical Flat Plate

S. F. Ahmmed[1], S. Mondal[2], A. Ray[3]
1, 2, 3 Mathematics Discipline, Khulna University, Bangladesh

ABSTRACT: *We investigate the two dimensional free convection and mass transfer flow of an incompressible, viscous and electrically conducting fluid past a continuously moving vertical flat plate in the presence of heat source, thermal diffusion, large suction and the influence of uniform magnetic field applied normal to the flow. Usual similarity transformations are introduced to solve the momentum, energy and concentration equations. To obtain the solutions of the problem, the ordinary differential equations are solved by using perturbation technique. The expressions for velocity field, temperature field, concentration field, skin friction, rate of heat and mass transfer have been obtained. The results are discussed in detailed with the help of graphs and tables to observe the effect of different parameters.*

Keywords: *Free convection, MHD, Mass transfer, Thermal diffusion, Heat source parameter.*

I. INTRODUCTION

Magneto-hydrodynamic (MHD) is the branch of continuum mechanics which deals with the flow of electrically conducting fluids in electric and magnetic fields. Many natural phenomena and engineering problems are worth being subjected to an MHD analysis. Furthermore, Magneto-hydrodynamic (MHD) has attracted the attention of a large number of scholars due to its diverse applications.

In engineering it finds its application in MHD pumps, MHD bearings etc. Workers likes Hossain and Mandal [1] have investigated the effects of magnetic field on natural convection flow past a vertical surface. Free convection flows are of great interest in a number of industrial applications such as fiber and granular insulation, geothermal systems etc. Buoyancy is also of importance in an environment where differences between land and air temperatures can give rise to complicated flow patterns.

Convection in porous media has applications in geothermal energy recovery, oil extraction, thermal energy storage and flow through filtering devices. The phenomena of mass transfer are also very common in theory of stellar structure and observable effects are detectable, at least on the solar surface. The study of effects of magnetic field on free convection flow is important in liquid-metal, electrolytes and ionized gases. The thermal physics of hydro-magnetic problems with mass transfer is of interest in power engineering and metallurgy. The study of flows through porous media became of great interest due to its wide application in many scientific and engineering problems. Such type of flows can be observed in the movement of underground water resources, for filtration and water purification processes, the motion of natural gases and oil through oil reservoirs in petroleum engineering and so on. The porous medium is in fact a non-homogeneous medium. The velocity is usually so small and the flow passages are so narrow that laminar flow may be assumed without hesitation. Rigorous analysis of the flow is not possible because the shape of the individual flow passages is so varied and so complex. Poonia and Chaudhary [2] studied about the flows through porous media. Recently researchers like Alam and Rahman [3], Sharma and Singh [4] Chaudhary and Arpita [5] studied about MHD free convection heat and mass transfer in a vertical plate or sometimes oscillating plate. An analysis is performed to study the effect of thermal diffusing fluid past an infinite vertical porous plate with Ohmic dissipation by Reddy and Rao [6]. The combined effect of viscous dissipation, Joule heating, transpiration, heat source, thermal diffusion and Hall current on the hydro-Magnetic free convection and mass transfer flow of an electrically conducting, viscous, homogeneous, incompressible fluid past an infinite vertical porous plate are discussed by Singh *et. al.* [7]. Singh [8] has also studied the effects of mass transfer on MHD free convection flow of a viscous fluid through a vertical channel walls. An extensive contribution on heat and mass transfer flow has been made by Gebhart [9] to highlight the insight on the phenomena. Gebhart and Pera [10] studied heat and mass transfer flow under various flow situations. Therefore several authors, viz. Raptis and Soundalgekar [11], Agrawal *et. al.* [12], Jha and Singh [13], Jha and Prasad [14] have paid attention to the study of MHD free convection and mass transfer flows. Abdusattar [15] and Soundalgekar ET.

al. [16] also analyzed about MHD free convection through an infinite vertical plate. Acharya *et. al.*[17] have presented an analysis to study MHD effects on free convection and mass transfer flow through a porous medium with constant auction and constant heat flux considering Eckert number as a small perturbation parameter. This is the extension of the work of Bejan and Khair [18] under the influence of magnetic field. Singh [19] has also studied effects of mass transfer on MHD free convection flow of a viscous fluid through a vertical channel using Laplace transform technique considering symmetrical heating and cooling of channel walls. A numerical solution of unsteady free convection and mass transfer flow is presented by Alam and Rahman [20] when a viscous, incompressible fluid flows along an infinite vertical porous plate embedded in a porous medium is considered.

In view of the application of heat source and thermal diffusion effect, the study of two dimensional MHD free convection and mass transfer flow past an infinite vertical porous plate taking into account the combined effect of heat source and thermal diffusion with a great agreement was conducted by Singh ET. *al.*[21].

In our present work, the effect of large suction on MHD free convection heat and mass transfer flow past a vertical flat plate has been investigated by similarity solutions which are obtained by employing the perturbation technique. We have used MATHMATICA to draw graph and to find the numerical results of the equation.

II. THE GOVERNING EQUATIONS

Consider a two dimensional steady free convection heat and mass transfer flow of an incompressible, electrically conducting and viscous fluid past an electrically non-conducting continuously moving vertical flat plate.

Introducing a Cartesian co-ordinate system, x-axis is chosen along the plate in the direction of flow and y-axis normal to it. A uniform magnetic field is applied normally to the flow region. The plate is maintained at a constant temperature T_w and the concentration is maintained at a constant value C_w. The temperature of ambient flow is T_∞ and the concentration of uniform flow is C_∞.

Considering the magnetic Reynold's number to be very small, the induced magnetic field is assumed to be negligible, so that $\vec{B} = (0, B_0(x), 0)$. The equation of conservation of electric charge is $\nabla.\vec{J}$ Where $\vec{J} = (Jx, Jy, Jz)$ and the direction of propagation is assumed along y-axis so that J does not have any variation along y-axis so that the y derivative of $\vec{J}$ namely $\frac{\partial J_y}{\partial y} = 0$ resulting in J_y=constant.

Also the plate is electrically non-conducting J_y=0 everywhere in the flow. Considering the Joule heating and viscous dissipation terms to negligible and that the magnetic field is not enough to cause Joule heating, the term due to electrical dissipation is neglected in the energy equation.

The density is considered a linear function of temperature and species concentration so that the usual Boussinesq's approximation is taken as $\rho=\rho_0$ [1-{β (T-T_∞) +β^*(C-C_∞)}]. Within the frame work of delete such assumptions the equations of continuity, momentum, energy and concentration are following [21]

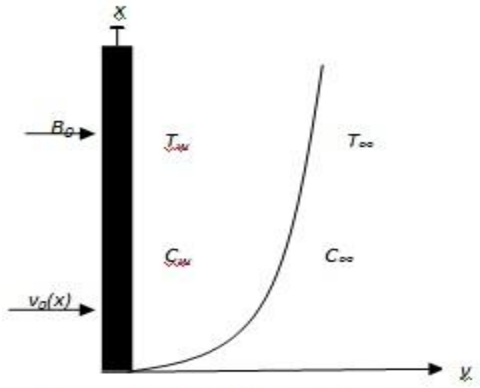

Fig.-Physical model of boundary layer

Continuity equation

$$\frac{\partial u}{\partial x} + \frac{\partial v}{\partial y} = 0 \tag{1}$$

Momentum equation

$$u\frac{\partial u}{\partial x} + v\frac{\partial v}{\partial y} = \vartheta\frac{\partial^2 u}{\partial y^2} + g\beta(T - T_\infty) + g\beta^*(C - C_\infty) - \frac{\sigma' B_0^2(x)}{\rho}u \tag{2}$$

Energy equation

$$u\frac{\partial T}{\partial x} + v\frac{\partial T}{\partial y} = \frac{K}{\rho C_p}\frac{\partial^2 T}{\partial y^2} + Q(T - T_\infty) \tag{3}$$

Concentration equation

$$u\frac{\partial C}{\partial x} + v\frac{\partial C}{\partial y} = D_M\frac{\partial^2 C}{\partial y^2} + D_T\frac{\partial^2 T}{\partial y^2} \tag{4}$$

The boundary conditions relevant to the problem are

$$u = U_0,\ v = v_0(x),\ T = T_w,\ C = C_w \ \text{ at } y = 0 \qquad u = 0,\ v = 0,\ T = T_\infty,\ C = C_\infty \ \text{ at } y \to \infty \tag{5}$$

Where u and v are velocity components along x-axis and y-axis respectively, g is acceleration due to gravity, T is the temperature. K is thermal conductivity, σ' is the electrical conductivity, D_M is the molecular diffusivity, U_0 is the uniform velocity, C is the concentration of species, $B_0(x)$ is the uniform magnetic field, C_P is the specific heat at constant pressure, Q is the constant heat source(absorption type), D_T is the thermal diffusivity, $C(x)$ is variable concentration at the plate, $v_0(x)$ is the suction velocity, ρ is the density, ϑ is the kinematic viscosity, β is the volumetric coefficient of thermal expansion and β^* is the volumetric coefficient of thermal expansion with concentration and the other symbols have their usual meaning. For similarity solution, the plate concentration $C(x)$ is considered to be $C(x)=C_\infty+(C_w-C_\infty)x$.

III. MATHEMATICAL ANALYSIS

We introduce the following local similarity variables of equation (6) into equation (2) to (4) and boundary condition (5) and get the equation (7) to (9) and boundary condition (10)

$$\psi = \sqrt{2\vartheta x U_0}\, f(\eta), \quad \eta = y\sqrt{\frac{U_0}{2\vartheta x}}, \tag{6}$$

$$\theta(\eta) = \frac{T - T_\infty}{T_w - T_\infty}, \quad \phi(\eta) = \frac{C(x) - C_\infty}{C_w - C_\infty}$$

$$f''' + ff' - Mf' + Gr\theta + Gm\phi = 0 \tag{7}$$

$$\theta'' + \Pr f\theta' - S\Pr\theta = 0 \tag{8}$$

$$\phi'' - 2Scf'\phi + Scf\phi' + S_0 Sc\theta'' = 0 \tag{9}$$

where $\Pr = \frac{\mu Cp}{k}$ is the Prandtl number,

$Gr = \frac{2xg\beta(T_w - T_\infty)}{U_0^2}$ is the Grashof number,

$\mathrm{Gm} = \frac{2xg\beta^*(C_w - C_\infty)}{U_0^2}$ is Modified Grashof number,

$S = \frac{2xQ}{U_0}$ is the Heat source paramater,

$M = \frac{2x\sigma'\beta_0^2(x)}{U_0\rho}$ is Magnetic parameter,

$Sc = \frac{\vartheta}{D_M y}$ is the Schmidt number and

$S_0 = \frac{T_w - T_\infty}{C_w - C_\infty}$ is the Soret number

with the boundary condition,

$$f = f_w, \quad f' = 1, \quad \theta = 1, \quad \phi = 1 \quad \text{at}\ \eta = 0 \tag{10}$$
$$f' = 0, \quad \theta = 0, \quad \phi = 0 \quad \text{as} \quad \eta \to \infty$$

where $f_w = v_o(x)\sqrt{\frac{2x}{\vartheta U_0}}$ and primes denotes the derivatives with respect to η.

$$\xi = \eta f_w, \quad f(\eta) = f_w X(\xi),$$

$$\theta(\eta) = f_w^2 Y(\xi), \quad \phi(\eta) = f_w^2 Z(\xi) \tag{11}$$

By using the above equation (11) in the equations (7) - (9) with boundary condition (10) we get,

$$X''' + XX'' = \varepsilon(MX' - GrY - GmZ) \tag{12}$$

$$Y'' + \Pr XY' = \varepsilon S\Pr Y \tag{13}$$

$$Z'' - 2ScZX' + ScXZ' + ScS_0 Y'' = 0 \tag{14}$$

The boundary conditions (10) reduce to

$$X = 1, \quad X' = \varepsilon, \quad Y = \varepsilon \quad \text{and}\ Z = \varepsilon \quad \text{at} \quad \xi = 0 \tag{15}$$
$$X' = 0, \quad Y = 0, \quad Z = 0 \quad \text{as} \quad \xi \to \infty$$

Now we can expand X, Y and Z in powers of ε as follows since $\varepsilon = \frac{1}{f_w^2}$ is a very small quantity for large suction

$$X(\xi) = 1 + \varepsilon X_1(\xi) + \varepsilon^2 X_2(\xi) + \varepsilon^3 X_3(\xi) + \ldots\ldots \tag{16}$$

$$Y(\xi) = \varepsilon Y_1(\xi) + \varepsilon^2 Y_2(\xi) + \varepsilon^3 Y_3(\xi) + \ldots\ldots \tag{17}$$

$$Z(\xi) = \varepsilon Z_1(\xi) + \varepsilon^2 Z_2(\xi) + \varepsilon^3 Z_3(\xi) + \ldots\ldots \tag{18}$$

Using equations (16)-(18) in equations (12)-(14) and considering up to order $O(\varepsilon^3)$, we get the following three sets of ordinary differential equations and their corresponding boundary conditions

First order $O(\varepsilon)$:

$$X_1''' + X_1'' = 0 \tag{19}$$

$$Y_1'' + \Pr Y_1' = 0 \tag{20}$$

$$Z_1'' + ScZ_1' + ScS_0 Y_1'' = 0 \tag{21}$$

The boundary conditions for 1st order equations are

$$X_1 = 0, X_1' = 1, \ Y_1 = 1, \ Z_1 = 1 \text{ at } \ \xi = 0 \tag{22}$$
$$X_1' = 1, \quad Y_1 = 0, \ Z_1 = 0 \quad \text{as} \quad \xi = 0$$

Second order $O(\varepsilon^2)$:

$$X_2''' + X_2'' + X_1 X_1'' = MX_1' - GrY_1 - GmZ_1 \tag{23}$$

$$Y_2'' + \Pr X_1 Y_1' + \Pr Y_2' = S\Pr Y_1 \tag{24}$$

$$Z_2'' + ScZ_2' = 2ScX_1'Z_1 - ScX_1 Z_1' - ScS_0 Y_2'' \tag{25}$$

The boundary conditions for 2nd order equations are

$$X_2 = 0, \quad X_2' = 0, \quad Y_2 = 0, \quad Z_2 = 0 \quad \text{at} \quad \xi = 0 \tag{26}$$
$$X_2 = 0, \quad Y_2 = 0, \quad Z_2 = 0 \quad \text{as} \quad \xi \to \infty$$

Third order $O(\varepsilon^3)$:

$$X_3''' + X_3'' + X_1'' X_2 X_1 X_2'' = MX_2' - GrY_2 - GmZ_2 \tag{27}$$

$$Y_3'' + \Pr X_1 Y_2' + \Pr X_2 Y_1' + \Pr Y_3' = S\Pr Y_2 \tag{28}$$

$$Z_3'' + ScZ_3' = 2ScX_1'Z_2 + 2ScX_2'Z_1 - ScX_2 Z_1' - ScX_1 Z_2' - ScS_0 Y_3'' \tag{29}$$

The boundary conditions for 3rd order equations are

$$X_3 = 0, \quad X_3' = 0, \quad Y_3 = 0, \quad Z_3 = 0 \quad \text{at} \quad \xi = 0 \tag{30}$$
$$X_3' = 0, \quad Y_3 = 0, \quad Z_3 = 0 \quad \text{as} \quad \xi = \infty$$

The solution of the above coupled equations (19) to (30) under the prescribed boundary conditions are as follows

First order $O(\varepsilon)$:

$$X_1 = 1 - e^{-\xi} \tag{31}$$

$$Y_1 = e^{-\Pr\xi} \tag{32}$$

$$Z_1 = (1 - A_1)e^{-Sc\xi} + A_1 e^{-\Pr\xi} \tag{33}$$

Second order $O(\varepsilon^2)$:

$$X_2 = \frac{1}{4}e^{-2\xi} + (A_7 + A_2\xi)e^{-\xi} - A_8 e^{-\Pr\xi} + A_9 e^{-Sc\xi} + A_{10} \tag{34}$$

$$Y_2 = (A_{11} - A_{12}\xi)e^{-\Pr\xi} - A_{11}e^{-(1+\Pr)\xi} \tag{35}$$

$$Z_2 = (B_5 - B_1 - B_2 - B_3 - B_6\xi)e^{-Sc\xi} + (B_3 - B_5 + B_4\xi) e^{-\Pr\xi} + B_1 e^{-(1+\Pr)\xi} + B_2 e^{-(1+Sc)\xi} \tag{36}$$

Third order $O(\varepsilon^3)$:

$$X_3 = B_{31} + (B_{24} + B_{32}\xi + \frac{B_9}{2}\xi^2)e^{-\xi} - (\frac{B_7}{4} - A_2 - \frac{A_2}{2}\xi) e^{-2\xi} + (B_{25} + B_{26} + B_{18}\xi)e^{-\Pr\xi} - [B_{27} - B_{28} - B_{21}\xi] e^{-Sc\xi} - B_{29}e^{-(1+\Pr)\xi} - B_{30}e^{-(1+Sc)\xi} - \frac{1}{24}e^{-3\xi} \quad (37)$$

$$Y_3 = [B_{40} + B_{41}\xi + \frac{B_{34}}{2}\xi^2]e^{-\Pr\xi} + [B_{39} - B_{35} + B_{36}\xi]e^{-(1+\Pr)\xi} + B_{37}e^{-(2+\Pr)\xi} + B_{38}e^{-(\Pr+Sc)\xi} + \frac{A_8}{2}e^{-2\Pr\xi} \quad (38)$$

$$Z_3 = B_{122}e^{-Sc\xi} + (B_{116} + B_{97}\xi)e^{-(1+Sc)\xi} + (B_{117} + B_{100}\xi)e^{-(1+\Pr)\xi} + B_{102}e^{-(2+\Pr)\xi} + B_{103}e^{-(2+Sc)\xi} + B_{104}e^{-(\Pr+Sc)\xi} - B_{105}e^{-2\Pr\xi} - B_{106}e^{-2Sc\xi} + (B_{118} + B_{119}\xi - B_{110}\xi^2)e^{-\Pr\xi} \quad (39)$$

Using equations (16) to (18) in equation (11) with the help of equations (31) to (39) we have obtained the velocity, the temperature and concentration fields as follows

Velocity distribution

$$u = U_0 f'(\eta) = U_0 f_w^2 X'(\xi) = U_0[X_1'(\xi) + \varepsilon X_2'(\xi) + \varepsilon^2 X_3'(\xi)] \quad (40)$$

Temperature distribution

$$\theta(\eta) = f_w^2 Y(\xi) = Y_1(\xi) + \varepsilon Y_2(\xi) + \varepsilon^2 Y_3(\xi) \quad (41)$$

Concentration distribution

$$\phi(\eta) = f_w^2 Z(\xi) = Z_1(\xi) + \varepsilon Z_2(\xi) + \varepsilon^2 Z_3(\xi) \quad (42)$$

The main quantities of physical interest are the local skin-friction, local Nusselt number and the local Sherwood number. The equation defining the wall skin-friction as

$$\tau = \mu\left(\frac{\partial u}{\partial y}\right)_{y=0} \quad (43)$$

Thus from equation (40) the skin-friction may be written as

$$\tau \propto [f''(\eta)]_{\eta=0} = [1 + \varepsilon\{1 + A_7 - 2A_2 + A_8 pr^2 + A_9 Sc^2\} + \varepsilon^2\{B_9 - 2B_{32} + B_{24} - B_7 + 2A_2 - 2B_{18}\Pr + \Pr^2(B_{25} + B_{26}) - 2B_{21}Sc - Sc^2(B_{27} - B_{28}) - B_{29}(1+\Pr)^2 - B_{30}(1+Sc)^2 - \frac{3}{8}\}] \quad (44)$$

The local Nusselt number denoted by Nu and defined as

$$Nu = -\left(\frac{\partial T}{\partial y}\right)_{y=0} \quad (45)$$

Therefore using equation (41), we have

$$Nu \propto [\theta'(\eta)]_{\eta=0} = -\Pr + \varepsilon(A_{11} - A_{12}) + \varepsilon^2[(B_{41} - \Pr B_{40} - (1+\Pr)(B_{39} - B_{35}) + B_{36} - B_{37}(2+\Pr) - B_{38}(\Pr + Sc) - A_8\Pr] \quad (46)$$

The local Sherwood number denoted by Sh and defined as

$$Sh = -\left(\frac{\partial C}{\partial y}\right)_{y=0} \quad (47)$$

Hence from equation (42), we can write

$$Sh \propto [\phi'(\eta)]_{\eta=0} = -A_1\Pr - Sc(1 - A_1) + \varepsilon\{Sc(B_1 + B_2 + B_3 - B_5) - B_6 - \Pr(B_3 - B_5) + B_4 - B_1(1+\Pr) - B_2(1+Sc) + \varepsilon^2\{-B_{122}Sc - (1+Sc)B_{116} + B_{97} - (1+\Pr)B_{117} + B_{100} - B_{102}(2+\Pr) - B_{103}(2+Sc) - B_{104}(\Pr+Sc) + 2B_{105}\Pr + 2B_{106}Sc - B_{118}\Pr + B_{119}\} \quad (48)$$

IV. RESULTS AND DISCUSSION

To observe the physical situation of the problem under study, the velocity field, temperature field, concentration field, skin-friction, rate of heat transfer and rate of mass transfer are discussed by assigning numerical values to the parameters encountered into the corresponding equations. To be realistic, the values of Schmidt number (*Sc*) are chosen for hydrogen (*Sc*=0.22), helium (*Sc*=0.30), water-vapor (*Sc*=0.60), ammonia (*Sc*=0.78), carbondioxeid (*Sc*=0.96) at 25°C and one atmosphere pressure. The values of Prandtl number (*Pr*) are chosen for air (*Pr*=0.71), ammonia (*Pr*=0.90), carbondioxied (*Pr*=2.2), water (*Pr*=7.0). Grashof number for heat transfer is chosen to be *Gr*=10.0, 15.0, -10.0, -15.0 and modified Grashof number for mass transfer *Gm*=15.0, 20.0, -15.0, -20.0. The values *Gr*>0 and Gm>0 correspond to cooling of the plate while the value *Gr*<0 and *Gr*<0 correspond to heating of the plate.

The values of magnetic parameter (*M*=0.0, 0.5, 1.5, 2.0), suction parameter (f_w =3.0, 5.0, 7.0, 9.0), Soret number (S_0=0.0, 2.0, 4.0, 8.0) and heat source parameter (*S*=0.0, 4.0, 8.0, 12.0) are chosen arbitrarily.

The velocity profiles for different values of the above parameters are presented from Fig.-1 to Fig.-11. All the velocity profiles are given against η.

In Fig.-1 the velocity distributions are shown for different values of magnetic parameter *M* in case of cooling of the plate (*Gr*>0). In this figure we observe that the velocity decreases with the increases of magnetic parameter.

The reverse effect is observed in the Fig.-2 in case of heating of the plate (*Gr*<0). The velocity distributions are given for different values of heat source parameter *S* in case of cooling of the plate in the Fig.-3. From this figure we further observe that velocity decreases with the increases of heat source parameter. The opposite phenomenon is observed in case of heating of the plate in Fig.-4. In Fig.-5 the velocity distributions are depicted for different values of suction parameter f_w in case of cooling of the plate. Here we see that velocity decreases with the increases of suction parameter. The reverse effect is seen in case of heating of the plate in Fig.-6.

The Fig.-7 represents the velocity distributions for different values of Schmidt number *Sc* in case of cooling of the plate. By this figure it is noticed that the velocity for ammonia (*Sc*=0.78) is less than that of hydrogen (*Sc*=0.22) decreases with the increases of Schmidt number. The reverse effect is obtained in case of heating of the plate in Fig.-8. The Fig.-9 exhibits the velocity distributions for different values of Soret number S_0 in case of cooling of the plate. Through this figure we conclude that the velocity increases increasing values of Soret number. The opposite phenomenon is seen in case of heating of the plate from Fig.-10.

In Fig.-11 the velocity distributions are presented for different values of *M*, *S*, *Sc*, *Pr* and f_w in both case of cooling and heating of the plate where S_0 =0.0 and U_0=1.0.

It is noted that for externally cooled plate (*a*) an increase in *M* decreases the velocity field is observed by curves (*i*) and (*ii*); (*b*) an increase in f_w decreases the velocity field observed by curves (*i*) and (*iii*); (*c*) an increase in *S* decreases the velocity field observed by curves (*iii*) and (*iv*); (*d*) an increase in *Sc* decreases the velocity field observed by curves (*i*) and (*v*); (*e*) an increase in *Pr* decreases the velocity field is seen in the curves (*i*) and (*vi*); (*f*) all these effects are observed in reverse order for externally heated plate. All the velocity profiles attain their peak near the surface of the plate and then decrease slowly along *y*-axis. *i.e.* far away from the plate. It is clear that all the profiles for velocity have the maximum values at η=1.

The temperature profiles are displayed from Fig.-12 to Fig.-14 for different values of *Pr*, *S* and f_w against η.

We see in the Fig.-12 the temperature distributions for different values of Prandtl number *Pr*. In this figure we conclude that the temperature decreases with the increases of Prandtl number. This is due to fact that there would be a decrease of thermal boundary layer thickness with the increase of prandtl number. In Fig.-13 displays the temperature distributions for different values of heat source parameter *S*. In this figure it is clear that the temperature field increases with the increases of heat source parameter.

Fig.-14 is the temperature distributions for different values of *Pr*, *S*, f_w for *Gr*=10.0, *Gm*=15.0, *M*=0.0, S_0 =0.0 and *Sc*=0.22. In this figure it is obtained that an increases in *Pr* and *S* decreases the temperature field but an increases in of f_w increases the temperature field.

The profiles for concentration are presented from Fig.-15 to Fig.-17 for different values of S_0, *Sc* and f_w.

The Fig.-15 demonstrates the concentration distributions for different values of Soret number. It is noticed that the concentration profile increases with the increases of Soret number. Fig.-16 gives the concentration distributions for different values of suction parameter f_w. We are also noticed that the effects of increasing values of f_w decrease the concentration profile in the flow field. In Fig.-17 the concentration distributions are shown for different values of *Sc*, S_0 and f_w for *Gr*=10.0, *Gm*=15.0, *M*=0.0, *S*=2.0 and *Pr*=0.71. In this figure it is seen that the concentration field increases with the increases of Schmidt number *Sc*.

The concentration field also increases with the increases of Soret number S_0. The concentration field decreases with the increases of suction parameter f_w. All the concentration profiles reach to its maximum values near the surface of the vertical plate *i.e.* η=1 and then decrease slowly far away the plate *i.e.* as $\eta\rightarrow\infty$

The numerical values of skin-friction (τ) at the plate due to variation in Grashof number (*Gr*), modified Grashof number (*Gm*), heat source parameter (*S*), Soret number (S_0), magnetic parameter (*M*), Schmit number (*Sc*), suction parameter (f_w), and Prandtl number (*Pr*) for externally cooled plate is given in Table-1. It is observed that both the presence of *S* and S_0 in the fluid flow decrease the skin-friction in comparison to their absence. The increase of *M*, *Sc* and f_w decreases the skin-friction while an increase in *Pr*, *Gr* and *Gm* increase the skin-friction in the absent of *S* and S_0.

Table-2 represents the skin-friction for heating of the plate and in this table it is clear that all the reverses phenomena of the Table-1 are happened.

The numerical values of the rate of heat transfer in terms of Nusselt number (*Nu*) due to variation in Pandlt number (*Pr*), heat source parameter (*S*) and suction parameter (f_w) is presented in the Table-3. It is clear that in the absence of heat source parameter the increase in *Pr* decreases the rate of heat transfer while an increase in f_w increases the rate of heat transfer. In the presence of heat source parameter the increasing values of f_w also increases the rate of heat transfer while an increase in *Pr* decreases the rate of heat transfer. It is also clear that the rate of heat transfer decreases in presence of *S* than the absent of *S*.

Table-4 depicts the numerical values of the rate of mass transfer in terms of Sherwood number (*Sh*) due to variation in Schmit number (*Sc*), heat source parameter (*S*), Soret number (S_0), suction parameter (f_w) and Pandlt number (*Pr*). An increase in *Sc* or *Pr* increases the rate of mass transfer in the presence of *S* and S_0 while an increase in f_w decreases the rate of mass transfer.

V. FIGURES AND TABLES

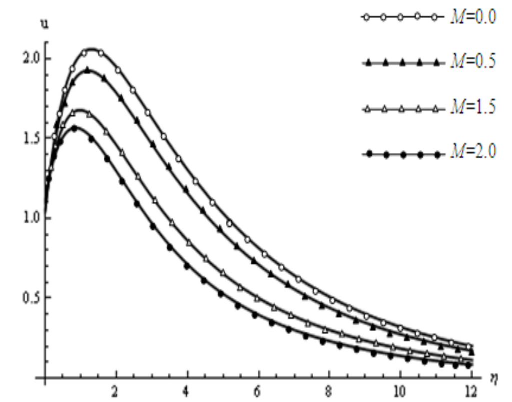

Fig.-1. Velocity profiles when *Gr*= 10.0, *Gm*= 15.0, *S*=0.0, S_0 =0.0, *Sc*=0.22, *Pr*=0.71, f_w=5.0 and U_0=1.0 against η.

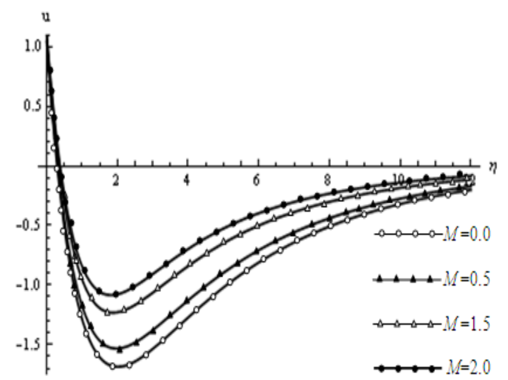

Fig.-2. Velocity profiles when Gr= -10.0, Gm= -15.0, S=0.0, S_0 =0.0, Sc=0.22, Pr=0.71, f_w=5.0 and U_0=1.0 against η

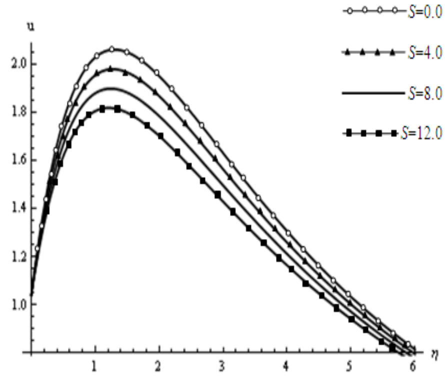

Fig.-3. Velocity profiles when Gr=10.0, Gm= 15.0, M=0.0, S_0=0.0, Sc=0.22, Pr=0.71, f_w=5.0 and U_0=1.0 against η.

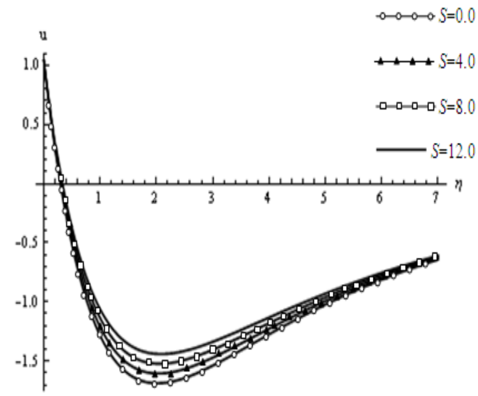

Fig.-4. Velocity profiles when Gr=-10.0, Gm=-15.0, M=0.0, S_0=0.0, f_w=5.0, Sc=0.22, Pr=0.71 and U_0=1.0 against η.

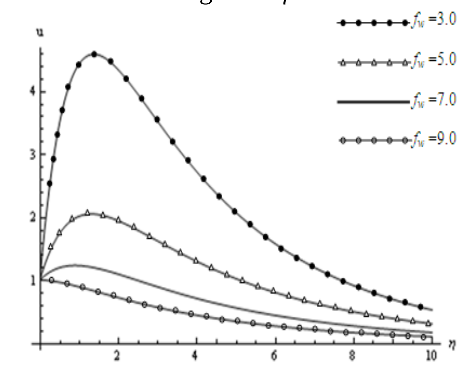

Fig.-5. Velocity profiles when Gr= 10.0, Gm= 15.0, M=0.0, S_0 =0.0, S=0.0, Sc=0.22, Pr=0.71 and U_0=1.0 against η.

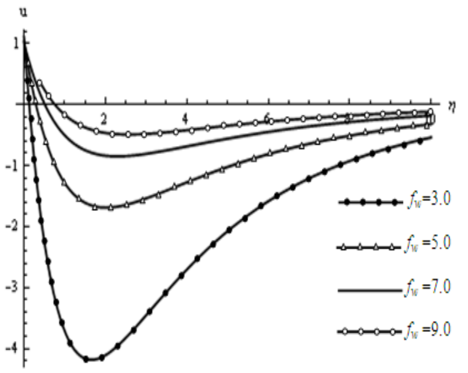

Fig.-6. Velocity profiles when Gr= -10.0, Gm= -15.0, M=0.0, S_0 =0.0, S=0.0, Sc=0.22, Pr=0.71 and U_0=1.0 against η.

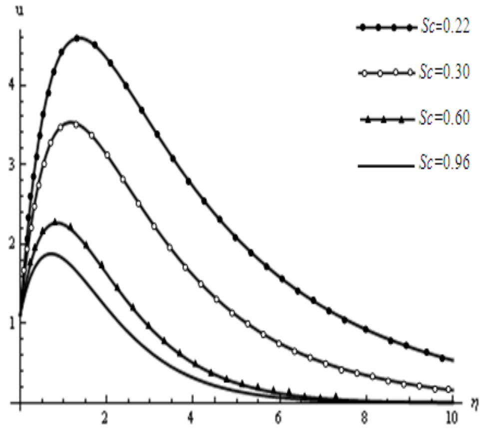

Fig.-7. Velocity profiles when Gr= 10.0, Gm= 15.0, M=0.0, S_0 =0.0, S=0.0, f_w =3.0, Pr=0.71 and U_0=1.0 against η.

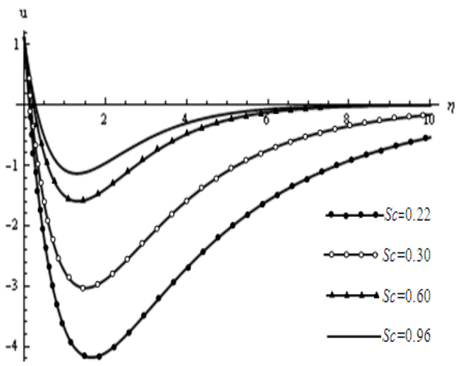

Fig.-8. Velocity profiles when Gr= -10.0, Gm= -15.0, M=0.0, S_0=0.0, S=0.0, f_w =3.0, Pr=0.71 and U_0=1.0 against η

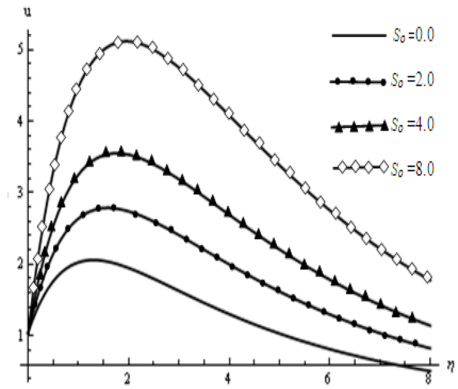

Fig.-9. Velocity profiles when Gr= 10.0, Gm= 15.0, M=0.0, S=0.0, Sc =0.22, f_w =5.0, Pr=0.71 and U_0=1.0 against η.

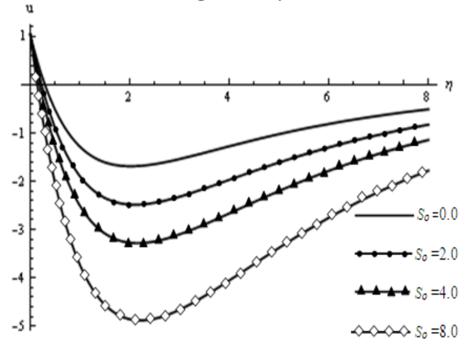

Fig.-10. Velocity profiles when Gr= -10.0, Gm= -15.0, M=0.0, S=0.0, f_w=5.0 , Sc =0.22

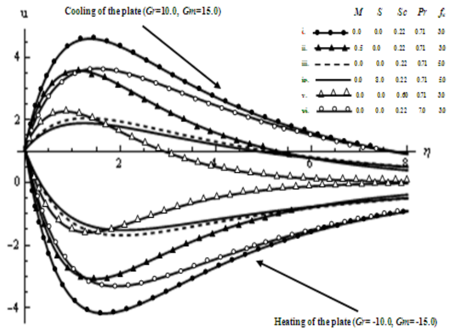

Fig.-11. Velocity profiles for different values of M, S, Sc, Pr and f_w when S_0 =0.0 and U_0=1.0 in both heating and cooling plate against η.

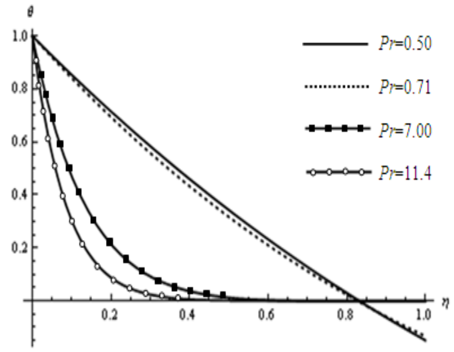

Fig.-12. Temperature profiles when Gr=10.0, Gm=15.0, M=0.5, S=1.0, S_0 =4.0, Sc=0.22 and f_w=3.0 against η.

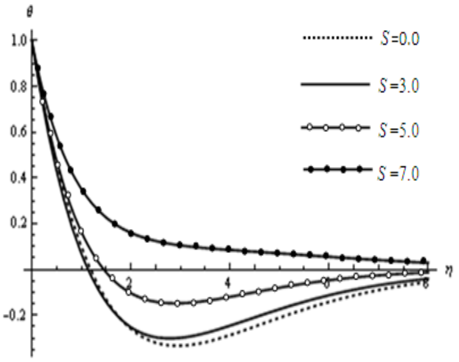

Fig.-13. Temperature profiles when Gr=10.0, Gm=15.0, M=0.0, S_0 =1.0, Sc=0.22, Pr= 0.71 and f_w=3.0 against η.

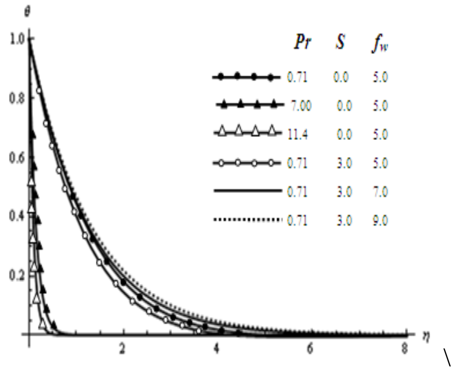

Fig.-14. Temperature profiles when Gr=10.0, Gm=15.0, M=0.0, S_0 =0.0 and Sc=0.22 against η.

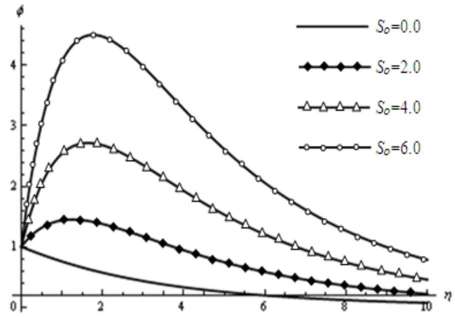

Fig.-15. Concentration profiles when Gr=10.0, Gm=15.0, S=0.0, M=0.5, Sc=0.22, Pr=0.71 and f_w=5.0 against η

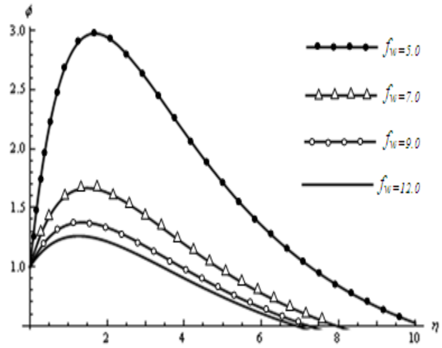

Fig.-16. Concentration profiles when Gr=10.0, Gm=15.0, S=4.0, M=0.0, S_0=4.0, Pr=0.71 an**d** Sc=0.22 against η

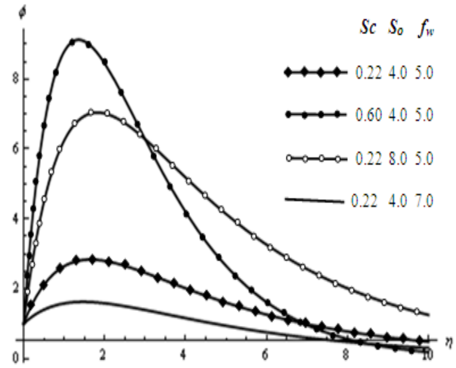

Fig.-17. Concentration profiles for different values of Sc, S_0 and f_w when Pr=0.71, M=0.0 and S =2.0 against η.

Table-1: Numerical values of Skin-Friction (τ) due to cooling of the plate.

S. No	Gr	Gm	S	S_0	M	Sc	f_w	Pr	T
1.	10.0	15.0	0.0	0.0	0.5	0.22	5	0.71	3.9187
2.	15.0	15.0	0.0	0.0	0.5	0.22	5	0.71	4.3051
3.	10.0	20.0	0.0	0.0	0.5	0.22	5	0.71	4.6694
4.	10.0	15.0	4.0	0.0	0.5	0.22	5	0.71	3.7917
5.	10.0	15.0	0.0	2.0	0.5	0.22	5	0.71	4.6313
6.	10.0	15.0	0.0	0.0	2.0	0.22	5	0.71	3.2845
7.	10.0	15.0	0.0	0.0	0.5	0.60	5	0.71	2.5551
8.	10.0	15.0	0.0	0.0	0.5	0.22	7	0.71	2.5571
9.	10.0	15.0	0.0	0.0	0.5	0.22	5	0.90	4.1025

Table-2: Numerical values of Skin-Friction (τ) due to cooling of the plate

S. No.	Gr	Gm	S	S_0	M	Sc	f_w	Pr	τ
1.	-10	-15	0.0	0.0	0.5	0.22	5	0.71	-2.131
2.	-15	-15	0.0	0.0	0.5	0.22	5	0.71	-2.517
3.	-10	-20	0.0	0.0	0.5	0.22	5	0.71	-2.881
4.	-10	-15	4.0	0.0	0.5	0.22	5	0.71	-2.004
5.	-10	-15	0.0	2.0	0.5	0.22	5	0.71	-2.843
6.	-10	-15	0.0	0.0	2.0	0.22	5	0.71	-1.809
7.	-10	-15	0.0	0.0	0.5	0.60	5	0.71	-0.767
8.	-10	-15	0.0	0.0	0.5	0.22	7	0.71	-0.662
9.	-10	-15	0.0	0.0	0.5	0.22	5	0.90	-2.314

Table-3: Numerical values of the Rate of Heat Transfer (*Nu*)

S. No.	Pr	S	f_w	Nu
1.	0.71	0.0	3	-1.3753
2.	0.71	4.0	3	-1.4886
3.	7.0	0.0	3	-7.2539
4.	7.0	4.0	3	-7.6531
5.	0.71	0.0	5	-0.8068
6.	0.71	4.0	5	-0.9232

Table-4: Numerical values of the Rate of Mass Transfer (*Sh*)

S. No.	Pr	S	S_0	f_w	Sc	Sh
1.	0.71	0.0	0.0	3	0.22	-0.5214
2.	0.71	4.0	2.0	3	0.22	7.4912
3.	0.71	0.0	2.0	3	0.22	6.5525
4.	0.71	4.0	2.0	3	0.60	111.935
5.	0.71	4.0	2.0	5	0.22	1.0846
6.	7.0	4.0	2.0	3	0.22	662.888
7.	0.71	8.0	4.0	3	0.22	25.3419

VI. CONCLUSION

In the present research work, combined heat and mass transfer effects on MHD free convection flow past a flat plate is presented. The results are given graphically to illustrate the variation of velocity, temperature and concentration with different parameters. Also the skin-friction, Nusselt number and Sherwood number are presented with numerical values for various parameters. In this study, the following conclusions are set out

(1) In case of cooling of the plate (Gr>0) the velocity decreases with an increase of magnetic parameter, heat source parameter, suction parameter, Schmidt number and Prandtl number. On the other hand, it increases with an increase in Soret number.

(2) In case of heating of the plate (Gr<0) the velocity increases with an increase in magnetic parameter, heat source parameter, suction parameter, Schmidt number and Prandtl number. On the other hand, it decreases with an increase in Soret number.

(3) The temperature increase with increase of heat source parameter and suction parameter. And for increase of Prandtl number it is vice versa.

(4) The concentration increases with an increase of Soret number and Schmidt number. Whereas it decreases with an increase of suction parameter.

(5) In case of cooling of the plate (Gr>0) the increase of magnetic parameter, Schmidt number and suction parameter decreases the skin-friction. While an increase of Grashof number, Modified Grashof number and Prandtl number increases the skin-friction. In case of heating of the plate (Gr<0) all the effects are in reverse order.

(6) The rate of heat transfer or Nusselt number (Nu) increase with the increase of suction parameter while an increase in Prandtl number it decreases. It also decreases in presence of S in comparison to absence of S.

An increase in Schmidt number or Prandtl number increases the rate of mass transfer (Sherwood number) in the presence of heat source parameter and Soret number while an increase in suction parameter f_w decreases the rate of mass transfer. We also see that both the increase in source parameter and Soret number increases the rate of mass

REFERENCES

[1] M. A. Hossain and A. C. Mandal, Journal of Physics D: Applied Physics, 18, 1985, 163-9
[2] H. Poonia and R. C. Chaudhary, Theoret. Applied Mechanics, 37 (4), 2010, 263-287
[3] M. S. Alam and M. M. Rahaman, Int. J. of Science and Technology, II (4), 2006
[4] P.R. Sharma and G. Singh, Int. J. of Appl. Math and Mech, 4(5), 2008, 1-8
[5] R. C. Chaudhary and J. Arpita, Roman J. Phy., 52(5-7), 2007, 505-524
[6] B. P. Reddy and J. A. Rao, Int. J. of Applied Math and Mech. 7(8), 2011, 78-97
[7] A. K. Singh, A. K. Singh and N.P. Singh, Bulletin of the institute of mathematics academia since, 33(3), 2005
[8] A. K. Singh, J. Energy Heat Mass Transfer, 22, 2000, 41-46
[9] B. Gebhart, Heat Transfer. New York: Mc Graw-Hill Book Co., 1971
[10] B. Gebhart and L. Pera, Ind. J. Heat Mass Transfer, 14, 1971, 2025–2050
[11] A. A. Raptis and V. M. Soundalgekar, ZAMM, 64, 1984, 127–130
[12] A. K. Agrawal, B. Kishor and A. Raptis, Warme und Stofubertragung, 24, 1989, 243–250
[13] B. K. Jha and A. K. Singh, Astrophysics. Space Science, pp. 251–255
[14] B. K. Jha and R. Prasad, J. Math Physics and Science, 26, 1992, 1–8
[15] M. D. Abdusattar, Ind. J. Pure Applied Math., 25, 1994, 259–266
[16] V. M. Soundalgekar, S. N. Ray and U. N Das, Proc. Math. Soc, 11, 1995, 95–98
[17] M. Acharya, G. C. Das and L. P. Singh, Ind. J. Pure Applied Math., 31, 2000, 1– 18
[18] A. Bejan and K. R. Khair, Int. J. Heat Mass Transfer, 28, 1985, 909–918
[19] A. K. Singh, J. Energy Heat Mass Transfer, 22, 2000, 41–46
[20] M. S. Alam and M. M. Rahman, BRACK University J. II (1), 2005, 111-115
[21] N. P. Shingh, A. K. Shingh and A. K. Shingh, the Arabian J. For Science and Engineering, 32(1), 2007.